

Polymer Growth by Functionalized Ruthenium Nanoparticles

Fei Ren, Alina K. Feldman, Matthew Carnes, Michael Steigerwald,* and Colin Nuckolls*

Department of Chemistry and The Columbia University Center for Electronics of Molecular Nanostructures, Columbia University, New York, New York 10027

Received August 13, 2007; Revised Manuscript Received August 16, 2007

ABSTRACT: We detail here a method to integrate reactive sites onto the surface atoms of ruthenium particles and use these sites as catalysts for oligomer growth. This way we can easily integrate nanoscale metal spheres both structurally and electronically with a shell of organic materials. We study the reaction of a zerovalent ruthenium precursor, Ru(η^4 -cyclooctadiene)(η^6 -cyclooctatriene), with different coordinating ligands. Using alcohol ligands produces large particles (~50 nm in diameter) that are composed of agglomerates of smaller particles. These particles are able to initiate olefin metathesis when they react with diazoalkanes and then strained olefins such as dicyclopentadiene, but the rates of reaction and number of active sites are low. When we use diazoalkanes directly without the intermediacy of the alcohol ligands, the activity of the particles increases, and we are able to produce particles that are as active as other heterogeneous olefin metathesis catalysts.

Introduction

It is challenging to integrate disparate materials such as small metal clusters (and their associated ligands) with polymers because each material has its own self-assembly characteristics. One method to embed particles within polymers is to grow multiple polymer chains from the surface of the particle.¹ In its most common form, this is achieved by tethering a known catalyst to the particle surface.^{2–10} While this is a useful technique, it would be valuable to be able to grow polymer directly from the surface of the particle.³ Here we explore this method by using the metal particle as the active catalyst.^{11,12} This allows us the opportunity to integrate nanoscale metal spheres both structurally and electronically with a shell of organic material.¹³ We focus on a reaction recently discovered for ruthenium films where they could be activated with monolayers of alkylidenes for olefin metathesis.¹³ We extend this reaction and install alkylidene sites into ruthenium nanoparticles (see Figure 1).^{14,15} These particles are able to perform ring-opening reactions with cyclic olefins to form living polymers that are attached to the particle surface.

Results and Discussion

Vidoni and co-workers have described the preparation of large Ru nanoparticles by the reaction of Ru(η^4 -cyclooctadiene)(η^6 -cyclooctatriene), **1**, with H₂ in a mixture of THF and methanol (19:1 by volume).^{16,17} Presumably, the hydrogen reacts with **1** to reduce the olefins to the noncoordinating, saturated hydrocarbons, leaving the nascent metal atoms to assemble into nanoclusters. In Figure 2 we show that this method produces nanoparticles of Ru that are quite large (average diameter = 56 nm), and the ensembles are quite polydisperse (± 29 nm). As others have noticed, a larger volume fraction of methanol in the reaction medium yields larger particles.^{16,17} Electron diffraction from these particles shows that they are hexagonally close-packed Ru. ¹H NMR of these samples prepared by centrifuging, washing, and drying shows only residual THF and methanol, with no trace of the cyclooctyl byproducts. We did not observe any upfield-shifted resonances characteristic of ruthenium hydrides in the NMR spectra of these particles.

* Corresponding authors. E-mail cn37@columbia.edu and mls2064@columbia.edu.

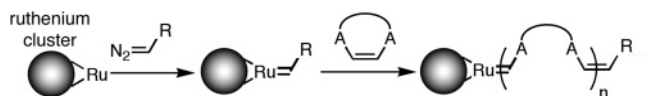


Figure 1. Metathesis growth of a polymer from a ruthenium particle activated with a substituted diazoalkane.

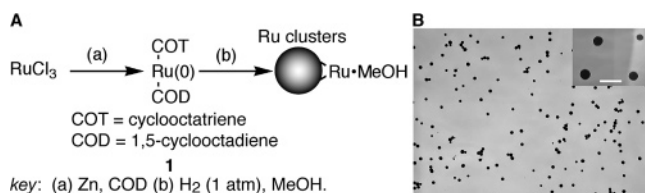


Figure 2. (A) Preparation of ruthenium clusters. (B) TEM image of ruthenium particles. Inset: higher magnification image. The scale bar is 100 nm.

These Ru nanoparticles do not react with even highly strained cyclic olefins at room temperature. This is consistent with previous observations regarding Ru surfaces.¹³ However, when the preformed particles are treated with trimethylsilyldiazomethane,¹⁵ the preformed particles are activated for reaction with strained olefins. In a typical experiment we hydrogenate **1** (40 mg, 0.13 mmol) in 30 mL of THF/MeOH (19:1), and after the particles form we add trimethylsilyldiazomethane, **2** (0.3–0.6 mL of a 2 M diethyl ether solution). The 1:2 molar ratio is between 1:5 and 1:10. These activated particles catalyze the polymerization of strained olefins. In Figure 3, we show TEM images of Ru particles after they have been treated with dicyclopentadiene (DCPD). It is noteworthy that upon polymerization of strained cyclic olefins TEM images of the product show that the particles (and, implicitly, the polymer coats) have coagulated. Analogous reactions of the activated particles with less strained cyclic olefins or acyclic olefins support this observation: with cyclo-octatetraene we observe only a negligible amount of clumping, and neither vinyltrimethylsilane nor acetylene causes any clumping at all. Micrographs of these latter cases are contained in the Supporting Information (Figure S1).

We propose that, as in the case of the two-dimensional Ru surface, the diazoalkane reacts with the particle surface, releasing N₂ and forming the functional equivalent of a surface alkylidene.¹⁸ The surface alkylidene is the active site for the ring-

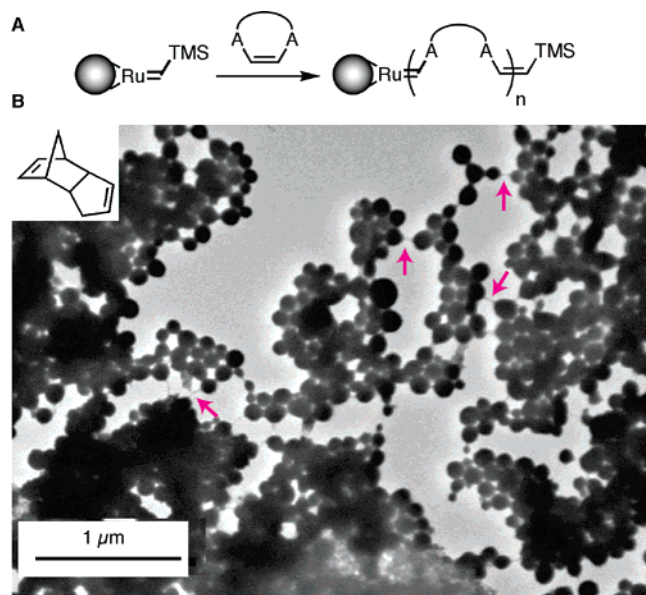


Figure 3. (A) Ring-opening metathesis reaction between a cyclic olefin and surface carbene. (B) Ring-opening metathesis with DCPD. The magenta arrows show areas where polymer is joining particles.

opening metathesis. As the polymers grow to surround their parent particles, phase separation occurs.

We compared the product of the nanoparticle-mediated polymerization of dicyclopentadiene (DCPD) with the polymer produced by the ROMP of DCPD using Grubbs' catalyst in CH_2Cl_2 at room temperature at low conversion controlled by triphenylphosphine.¹⁹ The ^1H NMR spectra of the two are essentially identical (see Supporting Information, Figure S2). Comparing the NMR of DCPD monomer and poly-DCPD, we find that the olefin peak correspond to the double bond in the bicyclic structure (5.95 ppm) disappears during polymerization as a group of broad peaks at higher field (5.3–5.7 ppm) begins to grow in. After 18 h the particle/polymer composite precipitates. This composite material is washed (to remove any solvent, soluble oligomers, and unreacted monomer) and dried to give a mechanically hard, black solid. Elemental analysis of this material (EDS) gives an elemental constitution of 1:2.67:0.08:0.08 (Ru:C:Si:O). Presuming each Si represents an active site, the C:Si ratio of ~ 33 indicates an average degree of DCPD oligomerization of 3. Since the NMR of the product shows the broadened resonances of higher oligomers and since TEM (Figure 3) shows particles surrounded and physically connected by organic material, we conclude that many of the sites labeled by Si are not productive, and very few sites are very active and result in high-molecular-weight polymers.

The apparent sparseness of productive sites may be due to several shortcomings of the method, but the large particle size is certainly significant. Nanoparticles of Ru prepared by this technique are not single crystalline; close examination of the TEM images shows that the particles are actually agglomerates of large numbers of much smaller (3–4 nm) clusters (see Supporting Information, Figure S3). While each of the small particles appears to be dense based on electron diffraction, the large particles are porous; i.e., there are voids between the constituent smaller clusters. It is reasonable to expect that a molecular reagent such as **2** could wend its way through these interstices of the agglomerate and react with the buried surface to form a buried alkylidene. Polymers growing from such buried active sites would soon choke the interstitial channels and thereby deactivate the catalytic sites. In order to forestall this,

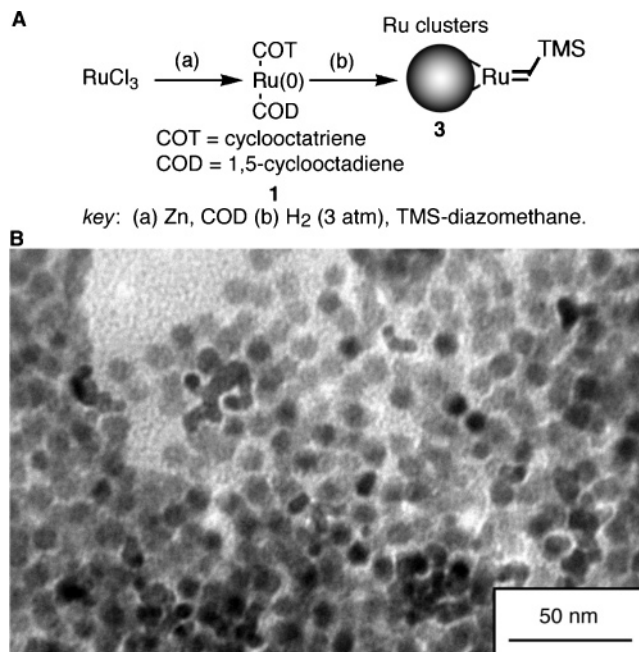


Figure 4. (A) Preparation of ruthenium clusters (**3**) with alkylidene linkages. (B) TEM image of ruthenium particles **3**.

we sought smaller, preferably dense and single-crystalline, Ru nanoparticles.

In the method of Ru particle formation presented by Vidoni et al.,^{16,17} methanol appears to act as a surface cap; it is critical to the formation and stabilization of the nanoparticle solution. When methanol is omitted from this preparation, a black solid (reported to be metallic ruthenium) precipitates irreversibly.^{16,17} We attempted to stabilize smaller nanoparticles by changing the THF/methanol ratio; this was unsuccessful. The replacement of methanol with alternative alcohols (pentanol, dodecanol, and *t*-butanol) did not give substantive changes—similar particle agglomerates formed. We replaced the alcohol with other ligands, those typically used to passivate late-metal clusters, but this was unsuccessful, albeit by giving “particles” that are far too small. For example, when ligands such as triethylphosphine or pyridine had been added to **1** and then hydrogenated in THF, we obtain a dark orange, homogeneous solution. These solutions are extremely air-sensitive; they turn dark green immediately when exposed to air, and in no case have we found evidence for nanoparticle formation. We believe these stronger ligands give mononuclear metal complexes such as $\text{Ru}(\text{C}_8\text{H}_{10})\text{L}_3$ (L = triethylphosphine or pyridine).^{20,21}

Reasoning that the alkylidene itself could act as at least a temporary surface cap, we examined the hydrogenation of **1** in the presence of **2**. This did give smaller Ru particles, forming solutions that are stable for several hours at room temperature. In a typical preparation, **1** (40 mg, 0.13 mmol) and **2** (0.06 mL of diethyl ether solution, 0.12 mmol) were combined in THF (30 mL), and H_2 (~ 3 atm) was introduced (Figure 4A). The color of the solution changed from yellow to dark brown, as it did in the methanol-containing process, during the formation of the Ru particles. After several hours these particles precipitate. When the solvent is removed and the resulting solid is exposed to air, it oxidizes quickly. In the time it takes to evaporate the material onto a TEM and transfer the grid to the microscope the particles partially oxidize; the electron diffraction shows hexagonally arranged RuO_2 as well as Ru. The TEM of these particles is shown in Figure 4B. Particles prepared in this way (**3**) are 10.3 ± 1.2 nm in diameter (Figure 4B).

Table 1. Summary of Molar Ratios of the Precursor to Initiator, Yield, Cis Ratio, Molecular Weight, and Polydispersity of Polynorbornene for Two Different Diazoalkane Initiators

	1:diazoalkane ^a	yield ^b (%)	σ_{cis} ^c	M_n ^d	P ^e
4-bromophenyldiazomethane	4:1	60	0.38	69 000	1.41
	1:1	>95	0.29	116 000	1.68
	1:3	>95	0.21	170 000	1.35
TMS-diazomethane	4:1	30	0.29	41 000	1.21
	1:1	>95	0.38	181 000	1.30
	1:10	>95	0.36	199 000	1.20

^a Ru:initiator refers to molar ratio between the ruthenium atoms and the diazoalkane. ^b Yield is the amount of the amount of alkene consumed relative to an internal standard. ^c σ_{cis} is the ratio of cis to trans double bonds formed in the polymerization. ^d M_n is the molecular weight determined by GPC comparing to polystyrene standards. ^e P is the polydispersity, $P = M_w/M_n$.

These smaller, “alkylidene-capped” Ru nanoparticles are much more active for ring-opening metathesis polymerization. To help understand the polymerization process, we analyze the formation of polynorbornene by TEM, NMR, and GPC. In a typical polymerization reaction, we mix 15 mL of a solution of **3** (approximately 6×10^{-5} mol Ru, 7×10^{-8} mol/L of particles) and the norbornene for 2 h at 65 °C. NMR confirms that the polymer is polynorbornene, identical to that produced with homogeneous catalysts.^{22,23} ¹H NMR shows the proton resonances at 5.23 and 5.36 ppm for the *cis*- and *trans*-olefinic protons. The ratio of cis vs trans olefin in this ring opening reaction is 0.379. ¹³C NMR consists of a group of upfield peaks assigned to the ring carbon atoms and a group of olefinic carbon peaks between 130 and 135 ppm. The conversion to polymer is high. For example, in the presence of 0.5 g of norbornene at 65 °C for 2 h in 15 mL of THF solution, the particles (approximately 6×10^{-5} mol Ru, 7×10^{-8} mol/L particle) produce polymer in >95% yield (see Table 1).

The nature of the diazoalkane has a pronounced effect on the rate of polymerization, the polymer microstructure, and the polydispersity of the polymer. Table 1 compares the yield, cis/trans ratio, molecular weight, and polydispersity of the polymer for various concentrations of two different diazoalkanes: TMS-diazomethane and 4-bromophenyldiazomethane. For both diazoalkanes the yield drops dramatically when the molar ratio of **1** to the diazoalkane is above 1:1. We speculate that the diazoalkane is needed to produce enough reactive sites on the surface of the particle. TMS-diazomethane tends to give lower polydispersity and higher molecular weights than 4-bromophenyldiazomethane. Both initiators give low-molecular-weight polymer at low initiator concentration and relatively high-molecular-weight polymer at higher concentration. The interpretation of how the cis ratio changes with the amount and constitution of the initiator is not clear. In the regime where the polymer yield is high, the TMS-diazomethane initiation provides twice as much *cis*-olefin as *trans*-olefin. For 4-bromophenyldiazomethane, we find the opposite. The σ_{cis} values decrease as the amount of initiator increases.

We monitor the kinetics of the polymerization process by synthesizing particles in THF-*d*₈ solution with TMS-diazomethane as the initiator and mesitylene as the internal standard (Figure 5). We mix a 1:1 molar ratio of Ru to initiator with 3 mg of initiator in 1 mL of THF-*d*₈ to monitor the reaction by NMR. The resulting solution is transferred into an NMR tube containing 20 mg of norbornene and 10 μ L of mesitylene and kept at 65 °C. The reaction is finished in less than an hour. The data within the first 40 min is in good correspondence with the first-order reaction of the monomer, and the rate constant

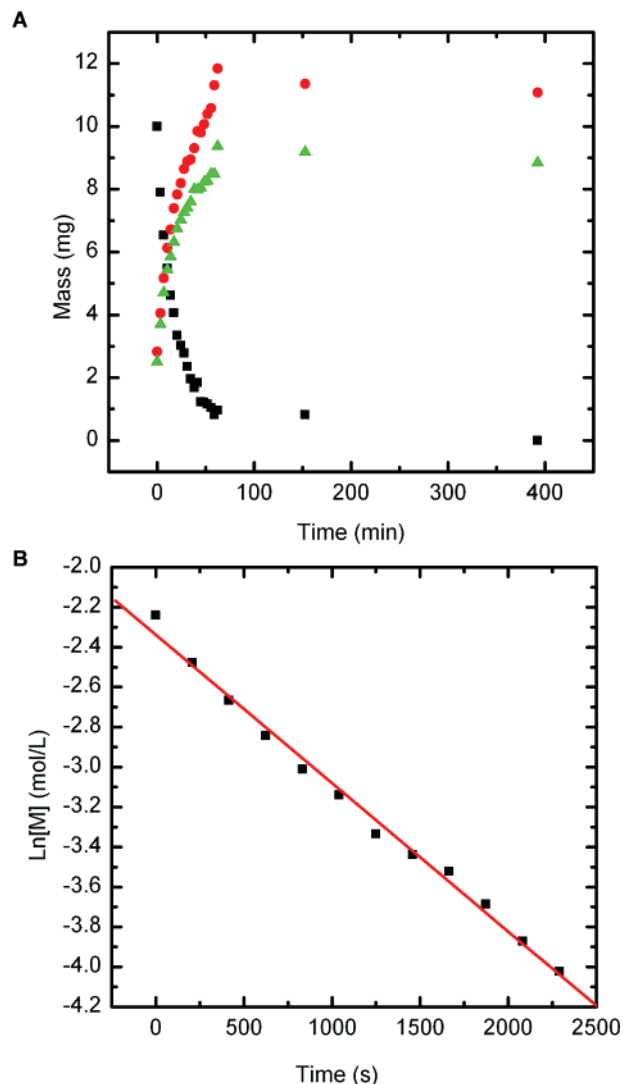


Figure 5. (A) Disappearance of norbornene (black squares) and the appearance of *trans* (red circles) and *cis* (green triangles) double bonds in relative to an internal standard (mesitylene) monitored by NMR. (B) Linear fit for the first-order reaction with rate constant $k = 7.4 \times 10^{-4} \text{ s}^{-1}$, $R^2 = 0.993$.

from the linear fit is $7.4 \times 10^{-4} \text{ s}^{-1}$. This value is comparable to olefin metathesis from other heterogeneous catalysts such as MoO_x ($8.3 \times 10^{-4} \text{ s}^{-1}$)²⁴ and $\text{WCl}_6/\text{SnMe}_4$ (7.2×10^{-4} – $2.3 \times 10^{-3} \text{ s}^{-1}$).²⁵ We can also add the monomer in several batches and see increases in rates. This indicates that during the polymerization reaction the ruthenium/alkylidene units are stable and active.

As the polymerization progresses, the solutions becomes viscous and a precipitate forms. The addition of ethyl vinyl ether (to quench the ROMP) and acetone gives copious amounts of white precipitate that darkens over time. Elemental analysis of the precipitate shows molar ratio 0.003:7.4:10.75 for Ru:C:H (corresponding to $\text{Ru}(\text{C}_7\text{H}_{10})_{350}$) before quenching and molar ratio 0.002:7.3:10.16 for Ru:C:H (corresponding to $\text{Ru}(\text{C}_7\text{H}_{10})_{520}$) after quenching. During quenching, polymer is detached from Ru particles, and the amount of Ru is reduced, but Ru particles remain embedded in the polymer matrix. The polymerization experiment can be performed in a flask open to air without any noticeable difference in yield and polymer structure. After centrifuging and drying, we obtain a black plastic solid, which does not redissolve in common organic solvents. Evaporation of solvent directly from the reaction solution results



Figure 6. (A) Polynorbornene solid formed by precipitation with methanol then centrifugation. (B) Polynorbornene film made by direct evaporation of the solvent.

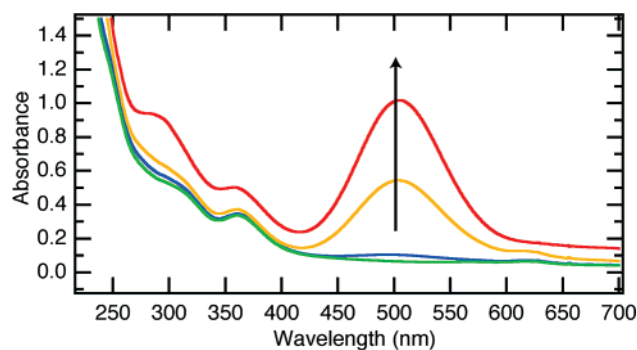


Figure 7. UV-vis absorbance spectrum of the oxidation of a polynorbornadiene film with I_2 vapor. Measurements were taken every 10 min.

in a brown, elastic film. Figure 6 shows images of this polynorbornene solid and film.

“Alkylidene-capped” particles, **3**, also catalyze the ROMP of both dicyclopentadiene (DCPD) and norbornadiene. In each case, as the reaction is kept at $65\text{ }^\circ\text{C}$ for 2 h, the brown solution of particles becomes viscous. After we centrifuge and dry the product of this reaction, we obtain a black hard solid, which does not redissolve in common organic solvents. For the poly-DCPD produced by **3**, GPC indicates $M_n = 46\ 000$ and a polydispersity of 3.6.

Polynorbornadiene (poly-NBD) is interesting because of its ability to form conjugated polymers.^{26,27} The poly-NBD produced by **3** has $M_n > 700\ 000$ and is highly polydisperse. Exposing either a solution or a thin film of the composite Ru particles integrated into poly-NBD to iodine at room temperature causes a rapid transformation of the polymer to a black, lustrous, and highly insoluble material. The process can be monitored by UV spectroscopy (Figure 7), where expected peaks at higher wavelength (namely, 290, 360, and 500 nm) grow as a function of time after the introduction of iodine. The exposure of poly-NBD to oxidizing agents dehydrogenates the polymer, creating regions of conjugated material. In the case of the integrated polymer-particle material, we find that such hydrogen abstraction reactions are more facile than in the case of the traditionally prepared sample of poly-NBD.²⁸ We believe that the metal particle aids in the oxidation of the attached polymer.

Conclusion

We have described a new reaction of transition-metal nanoparticles, the ring-opening metathesis polymerization of olefins. As in the previously reported reaction of Ru surfaces, this process is initiated by the reaction of diazoalkanes with the bare metal surface, in this instance the surface of the nanoparticle. The course taken by the polymerization depends strongly on how the nanoparticles are prepared, which ligand is used as the particle-capping agent, and which diazoalkane is used as the surface alkylidene source. We have studied the scope and limitations of this process, showing that in its present form the reaction occurs only with strained olefins; neither unstrained olefins nor acetylenes appear to react with the surface alkylidene. We have shown that the nanocrystalline metal particles can be incorporated into the polymer and that, in the case of polynorbornadiene, the polymer-bound particles can be used for subsequent transformations such as polymer dehydrogenation.

More broadly, this strategy described in the study represents a new type of catalytic system for polymerization, where the metal cluster or substrate participates in the catalysis while maintaining structural and electronic contact with the organic ligands. By adjusting the conjugation length of the material on the surface, we should be able to prepare electronic materials that are a composite of oligomers and metallic particles.

Acknowledgment. We acknowledge financial support from the Nanoscale Science and Engineering Initiative of the National Science Foundation under NSF Award CHE-0117752 and by the New York State Office of Science, Technology, and Academic Research (NYSTAR). We acknowledge support from the Chemical Sciences, Geosciences and Biosciences Division, Office of Basic Energy Sciences, US D.O.E. (#DE-FG02-01ER15264). C.N. thanks the Alfred P. Sloan Fellowship Program (2004). We thank the MRSEC Program of the National Science Foundation under Award DMR-0213574 and by the New York State Office of Science, Technology and Academic Research (NYSTAR) for financial support for MLS and the shared instrument facility. We also thank Dr. Cristian Grigoras (Columbia University) for assistance with the GPC samples.

Supporting Information Available: Details of the synthetic methods used, TEM images with different monomers, and details for the kinetics data. This material is available free of charge via the Internet at <http://pubs.acs.org>.

References and Notes

- Wang, J.-Y.; Chen, W.; Liu, A.-H.; Lu, G.; Zhang, G.; Zhang, J.-H.; Yang, B. *J. Am. Chem. Soc.* **2002**, *124*, 13358–13359.
- Hirai, T.; Watanabe, T.; Komasa, I. *J. Phys. Chem. B* **2000**, *104*, 8962–8966.
- Rutenberg, I. M.; Scherman, O. A.; Grubbs, R. H.; Jiang, W.; Garfunkel, E.; Bao, Z. *J. Am. Chem. Soc.* **2004**, *126*, 4062–4063.
- Skaff, H.; Ilker, M. F.; Coughlin, E. B.; Emrick, T. *J. Am. Chem. Soc.* **2002**, *124*, 5729–5733.
- Liu, X.; Basu, A. *J. Organomet. Chem.* **2006**, *691*, 5148–5154.
- Chabanas, M.; Copéret, C.; Basset, J.-M. *Chem.—Eur. J.* **2003**, *9*, 971–975.
- Weck, M.; Jackiw, J. J.; Rossi, R. R.; Weiss, P. S.; Grubbs, R. H. *J. Am. Chem. Soc.* **1999**, *121*, 4088–4089.
- Mayr, M.; Wang, D.; Kroll, R.; Schuler, N.; Pruhs, S.; Furstner, A.; Buchmeiser, M. R. *Adv. Synth. Catal.* **2005**, *347*, 484–492.
- Lee, B. S.; Namgoong, S. K.; Lee, S.-g. *Tetrahedron Lett.* **2005**, *46*, 4501–4503.
- Buchmeister, M. R. *Adv. Polym. Sci.* **2006**, *197*, 137–171.
- Shephard, D. S.; Maschmeyer, T.; Johnson, B. F. G.; Thomas, J. M.; Sankar, G.; Ozkaya, D.; Zhou, W.; Oldroyd, R. D.; Bell, R. G. *Angew. Chem., Int. Ed.* **1997**, *36*, 2242–2245.

- (12) Hungria, A. B.; Raja, R.; Adams, R. D.; Captain, B.; Thomas, J. M.; Midgley, P. A.; Golovko, V.; Johnson, B. F. G. *Angew. Chem., Int. Ed.* **2006**, *45*, 4782–4785.
- (13) Tulevski, G. S.; Myers, M. B.; Hybertsen, M. S.; Steigerwald, M. L.; Nuckolls, C. *Science* **2005**, *309*, 591–594.
- (14) Demonceau, A.; Stumpf, A. W.; Saive, E.; Noels, A. F. *Macromolecules* **1997**, *30*, 3127–3136.
- (15) Delaude, L.; Demonceau, A.; Noels, A. F. *Curr. Org. Chem.* **2006**, *10*, 203–215.
- (16) Vidoni, O.; Philippot, K.; Amiens, C.; Chaudret, B.; Balmes, O.; Malm, J.-O.; Bovin, J.-O.; Senoq, F.; Casanove, M.-J. *Angew. Chem., Int. Ed.* **1999**, *38*, 3736–3738.
- (17) Pelzer, K.; Vidoni, O.; Philippot, K.; Chaudret, B.; Colliere, V. *Adv. Funct. Mater.* **2003**, *13*, 118–126.
- (18) Noels, A. F. *Angew. Chem., Int. Ed.* **2007**, *46*, 1208–1210.
- (19) Risse, W.; Grubbs, R. H. *Macromolecules* **1989**, *22*, 1558–1562.
- (20) Komiya, S.; Planas, J. G.; Onuki, K.; Lu, Z.; Hirano, M. *Organometallics* **2000**, *19*, 4051–4059.
- (21) Hirano, M.; Asakawa, R.; Nagata, C.; Miyasaka, T.; Komine, N.; Komiya, S. *Organometallics* **2003**, *22*, 2378–2386.
- (22) Katayama, H.; Yonezawa, F.; Nagao, M.; Ozawa, F. *Macromolecules* **2002**, *35*, 1133–1136.
- (23) Gilliom, L. R.; Grubbs, R. H. *J. Am. Chem. Soc.* **1986**, *108*, 733–42.
- (24) Suzuki, T.; Hayashi, S.; Hirai, T.; Tanaka, K.; Toyoshima, I. *J. Mol. Catal.* **1989**, *49*, L43–L46.
- (25) Patton, P. A.; McCarthy, T. J. *Macromolecules* **1984**, *17*, 2939–2940.
- (26) Gillan, E. M. D.; Hamilton, J. G.; Mackey, O. N. D.; Rooney, J. J. *J. Mol. Catal.* **1988**, *46*, 359–371.
- (27) Gillan, E. M. D.; Hamilton, J. G.; Rooney, J. J. *J. Mol. Catal.* **1989**, *50*, L23–L26.
- (28) Frey, D. A.; Hasegawa, M.; Marvel, C. S. *J. Polym. Sci., Part A: Polym. Chem.* **1963**, *1*, 2057–2065.

MA071827H